Vertebra Shape Classification using MLP for Content-Based Image Retrieval

Sameer Antani, L. Rodney Long, George R. Thoma
Communications Engineering Branch http://archive.nlm.nih.gov
Lister Hill National Center for Biomedical Communications
National Library of Medicine
8600 Rockville Pike, Bethesda, MD 20894

R. Joe Stanley
Department of Electrical and Computer Engineering
University of Missouri-Rolla
127 Emerson Electric Company Hall,
1870 Miner Circle, Rolla, MO 65409-0040
Email: stanleyr@umr.edu

***Abstract*— A desirable content-based image retrieval (CBIR) system would classify extracted image features to support some form of semantic retrieval. The Lister Hill National Center for Biomedical Communications, an intramural R&D division of the National Library of Medicine (NLM), maintains an archive of digitized x-rays of the cervical and lumbar spine taken as part of the second National Health and Nutrition Examination Survey (NHANES II). It is our goal to provide shape-based access to the digitized x-rays including retrieval on automatically detected and classified pathology, e.g., anterior osteophytes. This is done using radius of curvature analysis along the anterior portion, and morphological analysis for quantifying protrusion regions along the vertebra boundary. Experimental results are presented for the classification of 704 cervical spine vertebrae by evaluating the features using a multi-layer perceptron (MLP) based approach. In this paper, we describe the design and current status of the content-based image retrieval (CBIR) system and the role of neural networks in the design of an effective multimedia information retrieval system.**

I. Introduction

The general problem of developing algorithms for the automated or computer-assisted indexing of images by structural contents is a significant research challenge [1]. This is particularly so in the case of biomedical images, where the structures of interest are commonly irregular, and may be partially occluded. Examples are the images created by digitizing film x-rays of the human cervical and lumbar spines, digitized color slides of the uterine cervix, color endoscopy images, endoscopic ultra-sonography images, etc. Text data in the form of patient or survey data is commonly associated with biomedical images. Systems currently allow retrieval of image data through a text based query. Content-based image retrieval (CBIR) aims to allow researchers and medical practitioners access to the images directly by their content. We envisage that the development of a system that provides such access would have many applications in education, research, clinical trials, diagnosis, etc. For example, a medical school faculty member who is an expert in degenerative spine disease could query for examples of severe disc space narrowing for both sexes for the cervical spine; or a clinician could use it for searching for images similar to a patient's present image pathology or injury. However a critical component in this system is the automated detection and classification of the pertinent pathology for effective semantic indexing. Classification of pathology in biomedical images requires classifiers to be trained for the many variations that can be found in the general population.

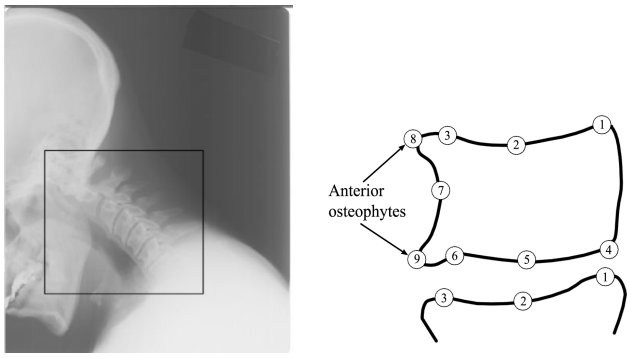

(a) (b)

Fig. 1. (a) Cervical spine x-ray example with region of interest. (b) Radiologist marked 9 points with anterior osteophytes labeled.

The Lister Hill National Center for Biomedical Communications, an intramural research and development division of the U.S. National Library of Medicine (NLM), maintains a digital archive of 17,000 cervical and lumbar spine images collected in the second National Health and Nutrition Examination Survey (NHANES II) conducted by the U.S. National Center for Health Statistics (NCHS). Along with the 10,000 cervical spine and 7,000 lumbar spine images, the NHANES II survey also included information on demographics, health questionnaire responses and physician's examination results. Over 2,000 fields of information are available on each surveyed person, providing a large body of text information. Figure 1(a) shows an example of the cervical spine image with the region of interest marked by a box. Figure 1(b) illustrates the locations of 9 landmark points marked by a radiologist. Presence of points 8 and/or 9, if marked on a vertebra, is indicative of anterior osteophytes.

Classification of the images for biomedical researchers, in particular the osteoarthritis research community, has been a long-standing goal of researchers at the NLM, collaborators at NCHS, and the U.S. National Institute of Arthritis and Musculoskeletal and Skin Diseases (NIAMS), and capability to retrieve images based on geometric characteristics of the vertebral bodies is of interest to the vertebral morphometry community. In this paper we describe the use of multi-layer perceptron (MLP) based classifiers in the prototype content-based image retrieval system [2], CBIR2, that also supports hybrid image and text queries. Image queries are posed by

0-7803-7898-9/03/$17.00 ©2003 IEEE

image-example or user-sketch. In addition to the CBIR2 built as a research tool, we have also developed a Web-based Medical Information Retrieval System (WebMIRS) to permit Internet access to databases of x-ray images and associated text data from NHANES [3]. Part of the initiative to develop WebMIRS is to determine the feasibility of computer-assisted techniques for the analysis of spine x-ray images. Radiographs of spine provide a practical approach for detecting and assessing vertebral abnormalities that may be related to osteoarthritis. The presence of bony growths on vertebra corners, viz., osteophytes, disc space narrowing, spondylolisthesis and subluxation are all features commonly evaluated visually from radiographs that are important to the osteoarthritis research community. Vertebral morphometry is a commonly used technique to evaluate these conditions. In particular, morphometric measurements of vertebral deformities are often used in clinical trials for assisting in the diagnosis and follow-up of fractures. Measurement techniques include conventional rulers and calipers [4], [5] and digitizing tablets [6], [7]. Morphometric analysis has encompassed radiographic diagnosis of vertebral fractures based on subjective visual assessment and arbitrarily assessed reductions in vertebral heights [8]. Prior studies have utilized vertebral dimensions to establish normal ranges using anterior and posterior vertebral height, percent reduction of anterior compared to posterior height of the same vertebra, the difference in vertebral height of adjoining vertebras, vertebral width, wedge angle and vertebra angle [4].

This research focuses on vertebra distortion along the anterior boundary as an indicator of osteophytes. Osteophyte presence is significant because it may be related to degeneration in the attachment of the outer annular fibers of the disc to the vertebral endplate. This degeneration may allow the vertebra to slip to the anterior or to both the anterior and the side [9]. In prior research we have investigated image processing techniques to compute features along the anterior boundary of cervical spine vertebrae for differentiating normal from fractured vertebrae [10]. As the vertebra becomes less normal in appearance, the vertebra boundary increasingly deviates from the general rectangular shape, which may be indicative of a vertebral fracture. The features examined were radius of curvature- and grayscale gradient-based features computed along the anterior boundary of cervical spine vertebrae. The radius of curvature-based features explore the relative constriction along the anterior boundary between normal and abnormal vertebrae. The grayscale border gradient features examine the grayscale contrast difference between the vertebra interior and exterior along the boundary. Preliminary results indicated potential utility in applying these features for osteophyte detection.

In this research, we extend the preliminary results to a substantial data set for evaluating the radius of curvature and boundary gradient features. We also introduce a morphological approach for detecting osteophytes. The morphology-based features utilize the binary opening operation to identify protrusion regions corresponding to constrictions along the anterior boundary. A standard multilayer perceptron (MLP) is used to evaluate the features for classifying cervical spine vertebrae as containing osteophytes or not. The size of the protrusion regions is used for differentiating normal and abnormal vertebrae. We present methods involved in the process and place them in the design of the CBIR2 multimedia information retrieval system. The design of CBIR2 is presented in Section II. The image analysis and vertebra recognition approach is presented in Section III. The experimental results are presented in Section IV. We conclude by describing our current status and outlining future work .

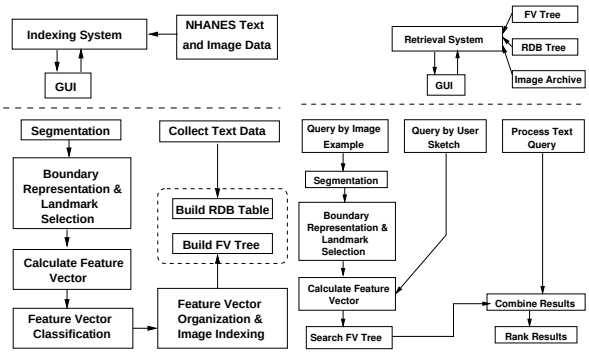

Fig. 2. CBIR2 Architecture

II. Design of CBIR2 system

In this section we describe the design architecture of our current prototype content-based image retrieval system, CBIR2. The system is modular and is logically composed of the indexing system and the retrieval system. The indexing system includes methods for automated image segmentation, image feature extraction, feature vector computation, feature classification, feature organization, image indexing, and text data organization. The retrieval system provides the interface and the methods for image and text retrieval including methods for extracting features from example images, computing the feature vector, and determining similarity between features extracted from the query visual and those stored in the database. In addition, text retrieval via SQL and methods to combine the text and image queries are included. The text data includes the patient survey data acquired in NHANES II as well as the results of the vertebra image analysis and recognition process described here. The architectures for the indexing and retrieval systems are shown in Figure 2.

A. Indexing system

The indexing process is currently semi-automated and done via a graphical interface. This interface allows indexing of two types of data. The text data is organized as fields in a relational database table from which data can be retrieved using the MySQL relational database manager. The indexing of the image data on the other hand is a more involved process. The system modules are briefly described.

I **Segmentation:** The first step in indexing the x-ray images is segmenting the vertebrae. The image quality in the

spine x-ray images is fairly poor with ambiguous vertebral boundaries, making a reliable segmentation a challenging task. Active Contour Segmentation (ACM) [11] and Active Shape Modelling (ASM) [12] techniques have been explored for segmenting the vertebrae. The segmentation output, which includes the template and segmentation results for each object, is stored in a XML file. This enables modifications following future developments. The file records the information about an image, database source, view (e.g., lateral, sagittal, AP), coordinate systems and origin, and the human segmentor in the header structure. The segmented objects are stored with a unique object identifier, anatomy identifiers, region of the anatomy, the segmented boundary points, the bounding box, the oriented bounding box, etc.

II **Feature extraction and representation** The vertebra boundary points extracted as (x, y) coordinates in the image space need to be represented in a form suitable for archiving, classification, indexing, and similarity matching by a shape representation algorithm. For matching and indexing, the coarse boundary and a binary image representation of the vertebra are used to find meaningful shape features that are invariant to translation, rotation, scaling and starting-point shift. Classification of vertebrae for pathology is also done using the boundary data.

III **Feature organization**
A feature vector is then created from various computed features and organized into a data structure for efficient retrieval. The development of a feature organization strategy is strongly correlated with the feature vector used, the query types supported, and the image semantics. We are at a stage where we have some of the these requirements identified. We are currently using a flat structure and linear search for retrieval. Having an inefficient but working system enables us to simultaneously test the system and improve on individual modules.

IV **Feature classification** Our work toward the indexing of spine images for features of interest in the osteoarthritis and vertebral morphometry research communities requires the segmentation of the images into vertebral structures with sufficient accuracy to distinguish pathology on the basis of shape, labeling of the segmented structures by proper anatomical name, and classification of the segmented, labeled structures into groups corresponding to high level semantic features of interest. Using training data provided by biomedical experts, we have adopted a hierarchical approach to such indexing that consists of high-level region classification, spine region localization, vertebra localization and identification, vertebral segmentation, and classification of the vertebrae by presence/absence of the biomedical features above [10], [13].

B. Retrieval system

The retrieval system provides an interface for the user to use the CBIR system. Many of the methods in this system are identical to those in the indexing system. The inputs to the retrieval system can be an image, for query by image example, or a shape, for query by shape. This is in addition to any text parameters.

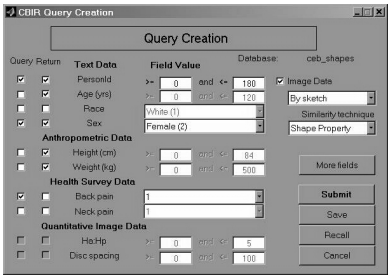

Fig. 3. Query Dialogs: Main Screen

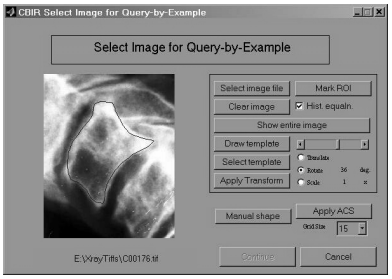

Fig. 4. Query Dialogs: Query-by-example.

The CBIR2 prototype system is implemented in MATLAB version 6.5. The basic types of queries supported are to the text data, image data and combined queries to both. The retrieval of the text data is supported through Open-Database Connectivity (ODBC) protocol to retrieve results using the MySQL DBMS. The queries to the image data can be specified in using an example image to retrieve images that are visually similar or by drawing a sketch of the indexed feature, in this case the vertebra boundary. The system presents the user with a GUI for creating queries and supports text, image example, and image sketch queries, and queries that combine text and image example or image sketch.

Figure 3 shows the initial screen for generating the basic query. The retrieval paths for image-example based queries and sketch-based queries are the same except for the feature extraction phase necessary for the former.

The same feature extraction phase as in the indexing process is applied to the example image. The user is presented with the ACS tool for segmenting the image. The extracted image features in the query are then matched by a shape similarity algorithm to determine the similarity distance between the query and the database shape. The greater the distance between two feature vectors the greater is the dissimilarity. The system allows users to specify an image for an image-example based query as shown in Figure 4. For a sketch-based query, the users may choose to either use one of the provided templates, or use their own template and modify it or draw an outline from scratch, as shown in Figure 5.

It is also possible to narrow the query to the segmentation done by a particular algorithm. Additionally, with several shape representation methods included, the user can also query

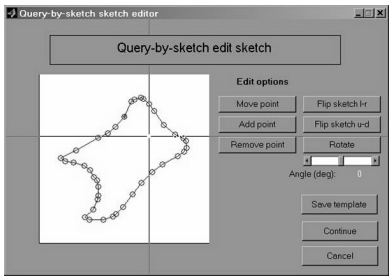

Fig. 5. Query-by-Sketch (User Sketch)

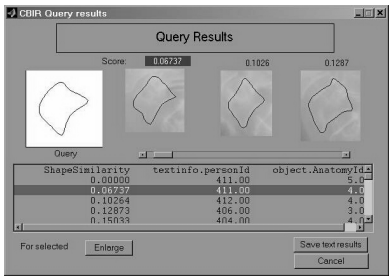

Fig. 6. CBIR2 Results

on a specific representation. The results from the query are presented as shown in Figure 6.

III. Vertebra Image Analysis and Recognition

We present image analysis and recognition techniques for detecting presence of osteophytes in cervical spine vertebrae.

A. **Vertebra Boundary Determination.** In order to detect the presence of osteophytes, it is necessary to segment the vertebra boundary. Histogram analysis based contrast enhancement techniques based on a two-tiered Gaussian-based thresholding approach [14] was used to determine lower and upper threshold bounds for approximating the intermediate region of the gray-scale image histogram. Threshold relaxation is performed to avoid oversegmenting the region containing the vertebrae. Histogram equalization is performed over the thresholded region containing the vertebrae for enhancing the contrast between the vertebrae and the surrounding regions. From the enhanced image, an edge magnitude image is determined using the Kirsch operator [15] to assist in determining vertebrae boundary. The edge magnitude and 9 radiologist marked landmark points are used to manually mark a preliminary set of boundary points. A B-spline algorithm was applied to this set to obtain a detailed boundary representation. Based on experimentation approximately 55 manually chosen points provided reasonable vertebra boundary representations for feature analysis. Typically, the B-Spline algorithm generates about 100-150 boundary points that are included in the region of interest. Sample results from these steps are shown in Figure 7.

B. **Radius of Curvature Feature Calculation** Radius of curvature- and border grayscale gradient-based features are computed on the anterior boundary of the vertebra. A region of interest boundary is selected from the segmented boundary. This region extends from the top center of the vertebra, around the anterior side to the bottom center. Both centers are from the radiologist marked points. The boundary is shown in Figure 8(a). Radius of curvature-based features are quantified along the region of greatest constriction along the vertebra's anterior boundary for identifying potential osteophytes. Osteophytes tend to exhibit greater constriction around the anterior top and bottom areas.

A least squares algorithm using 20 points on either side of a boundary point is applied to determine the radius of curvature for each boundary point. In addition, the row and column positions corresponding to the center of the projected circle is also computed. The features are determined using the sequence (or array) of radii of curvature computed along the vertebra boundary in the region of interest. These include: 1) radius of curvature at the boundary point, 2) first and 3) second derivatives of the radius of curvature at every point on the boundary. There are 27 radius of curvature features used for vertebra classification are formed with these three features at the 9 minimum radii of curvature along the boundary.

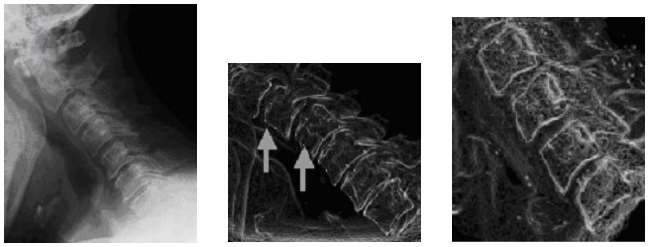

(a) (b) (c)

Fig. 7. Sample results from (a) histogram equalization (b) boundary points from Kirsch operator, and (c) B-spline fit to the boundary points.

C. **Boundary Gradient Features.** The region of interest along the anterior boundary provides the basis for grayscale gradient features. The grayscale gradient-based features quantify the transition in gray level from the interior of the vertebra boundary to the exterior of the vertebra boundary for each vertebra boundary point in the region of interest. The gradient-based features are used for discerning if the gray level information near the boundary of the vertebra differs between normal and abnormal vertebrae. These features are computed between 2 interior and 2 exterior points along the perpendicular directional line between the projected circle centers for each boundary point. The interior and exterior points must be 8 connected. The minimum, maximum, mean gradient value, its standard deviation are used as features. These points are shown in Figure 8(b).

D. **Morphology Feature Calculation.**
The maximum constriction region provides a small protrusion from the remainder of the vertebra. An alternative morphological approach for vertebra osteophyte detection has been investigated to isolate this protrusion region.

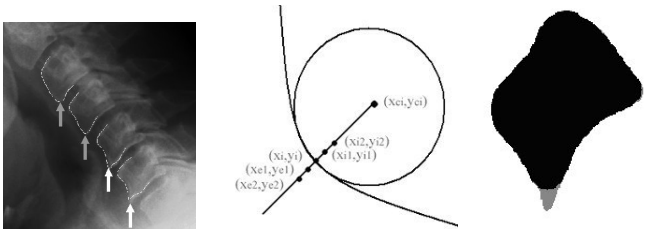

(a) (b) (c)

Fig. 8. (a) Anterior vertebra boundary, (b) points over which boundary gradient features are computed, and (c) area of largest protrusion identified after morphological operations.

This approach utilizes the opening operation with a large circular structuring element. An opening operation involves performing an erosion operation followed by a dilation operation using the same circular structuring element. An exclusive OR of the opened image with the vertebra image will identify the protrusion regions. We use the area of the largest protrusion region as the feature for for detecting osteophytes, shown in gray in Figure 8(c). It may be hypothesized that the region with the largest area will correspond to the region of maximum constriction along the vertebra boundary.

IV. Experiments Performed and Results

A. **Data Set Description.** 704 vertebrae from the cervical spine x-ray images are used as data. These include 352 normal vertebrae and 352 vertebrae with anterior osteophytes. Using the radiologist marked landmark points and the Kirsch edge-detected image as guides, approximately 55 points are manually selected along each vertebra's boundary, and then the B-Spline algorithm is used to generate a representation of the boundary as a continuous curve. The radius of curvature, border gradient and morphological features are determined based on these B-Spline representations of the vertebra boundaries.

B. **Structuring Element for Morphological Feature.** For the morphology feature, the size of the circular structuring element influences the effectiveness of the protrusion region extraction. A structuring element of radius 14 was empirically determined to be effective after evaluating several radii on a subset of the training data.

C. **Schemes for Vertebra Classification.** In order to evaluate the radius of curvature-, boundary gradient- and morphological-based features, two classification schemes are examined:

1. radius of curvature- and border gradient-based features are combined to generate a 31-feature vector for each vertebra,
2. radius of curvature-, border gradient- and morphological-based features are combined to generate a 32-feature vector for each vertebra.

Multi-layer perceptrons (MLP) are used as the classifiers for the feature vectors for classification schemes 1 and 2 above using a single output for vertebra class assignment.

	Training			Testing		
T	Normal	Abnorm.	Total	Normal	Abnorm.	Total
0.45	78.7	86.9	82.8	48.1	76.9	62.5
0.41	75.5	92.6	84.0	50.0	69.2	59.6
0.52	82.3	71.3	76.8	69.2	51.9	60.6
0.44	67.7	80.1	73.9	55.8	69.2	62.5
0.54	87.8	81.9	84.8	67.3	65.4	66.3
0.45	41.8	86.2	64.0	42.3	86.5	64.4
0.60	92.9	82.6	87.8	78.8	40.4	59.6
0.45	69.5	82.3	75.9	50.0	69.2	59.6
0.40	22.3	91.8	57.1	23.1	90.4	56.7
0.56	94.0	77.7	85.8	55.8	55.8	55.8
Avg.	71.2	83.3	77.3	54.0	67.5	60.8

TABLE I

Classification Results (% Correct) using 31-features. (T = T_{max31})

Data normalization for the 31- and 32-feature MLPs is based on computing the mean and standard deviation for each feature over the training set. For MLP training and testing, the feature vectors are normalized by subtracting the mean and dividing by the standard deviation for each feature. All data analysis was performed using MATLAB 6.1, including the built-in MLP functions used for neural network training and testing. For feature evaluation 15 training and testing sets were randomly chosen, using 80% of the data for training, 5% for cross-validation and the remaining 15% for testing.

564 vertebrae were used for training the MLPs and 106 vertebrae formed the testing set in this experiment. For each randomly chosen training, cross-validation and testing set, training for the 31- and 32-input feature MLPs is performed after each epoch. For cross-validation testing, we note the MLP cross-validation output threshold that yields the maximum percent correct vertebrae classification for the current epoch. The training is stopped at the maximum results in the cross-validation testing. T_{max} denotes the threshold at the epoch of MLP training. Thus, T_{max31} and T_{max32} refer to the thresholds for the current randomly chosen training, cross-validation and testing set for the 31- and 32-input feature MLPs, respectively.

A. Results

The neural network architectures used for feature evaluation were 31x15x15x1 and 32x15x1 for the 31- and 32-feature input MLPs, respectively. In the 31-feature neural network there are two hidden layers, each with 15 nodes, and one output node. In the 32-feature neural network there is one hidden layer with 15 nodes and one output node. For both networks for all training/testing set iterations, the following neural network parameters were used: learning rate of 0.03, momentum of 0.85, sigmoid transfer functions at the input and hidden layers, and a linear transfer function at the output layer. For each randomly chosen training, cross-validation and testing set, training is performed for the 31- and 32-feature MLPs using the procedure described above and thresholds T_{max31} and T_{max32} are determined. The median normal maximum protrusion region is found from the training set. The number of epochs used for MLP training is based on

	Training			Testing		
T	Normal	Abnorm.	Total	Normal	Abnorm.	Total
0.60	97.2	85.5	91.3	76.9	84.6	80.8
0.41	91.5	87.6	89.5	75.0	84.6	79.8
0.60	91.8	76.6	84.2	90.4	75.0	82.7
0.47	88.3	81.2	84.9	90.4	80.8	85.6
0.58	97.9	86.5	92.2	82.7	76.9	79.8
0.59	88.7	70.9	79.8	88.5	57.7	73.1
0.51	94.7	92.2	93.4	78.8	80.8	79.8
0.60	92.6	75.5	84.0	90.4	69.2	79.8
0.60	84.0	69.1	76.6	78.8	78.8	78.8
0.60	96.1	86.2	91.1	84.6	75.0	79.8
Avg.	92.3	81.2	86.7	83.7	76.3	80.0

TABLE II

CLASSIFICATION RESULTS (% CORRECT) USING 32 FEATURES. (T = T_{max32})

identifying the epoch for which the cross-validation results declined.

The classification schemes presented in "Schemes for Vertebra Classification" are evaluated for 10 randomly generated training/cross-validation/testing sets using 80% of the data for training, 5% for cross-validation and the remaining 15% of the data for testing. Table I shows the training and testing results over 10 iterations for the radius of curvature and border gradient features (31-feature case). Table II presents the training and testing results over 10 iterations for the radius of curvature, border gradient and morphological features (32 feature case). For each classification technique, the percentage of correctly classified normal vertebrae, abnormal vertebrae and total (normal and abnormal) are shown for all 10 randomly generated training/testing sets.

B. Analysis

The results fuel several observations. First, there are no significant differences between the training and testing results for the optimal MLP threshold. Second, the vertebrae with low grade abnormality often appear visually similar to normal vertebrae, making differentiation between the two classes difficult. Third, the vertebra normalization technique explored in this research may have impacted the classification results. Vertebra normalization needs to be performed for each level of vertebra rather than over the entire set. Finally, the radius of curvature and border gradient features performed much more poorly than the composite features (including the morphological feature) for vertebra classification. The average testing results from the radius of curvature and border gradient features from 60.08%, compared to 80.0% for the composite features. The radius of curvature and border gradient features do not contribute as significantly to correct vertebra classification as the morphological feature. One difficulty encountered with the radius of curvature features is that the least squares algorithm used for computing the radius of curvature and the center of the projected circle provides occasional noisy results, distorting the features. There are situations where the minimum radius of curvature along the vertebra anterior boundary is found at the correct location, but the radii of curvature computed in the neighboring positions are not consistent with the minimum radius of curvature found.

V. CONCLUSION AND FUTURE WORK

This paper describes results from an evaluation of MLP based vertebra classification schemes for detecting abnormal vertebrae in the cervical spine that have anterior osteophytes. This evaluation is a part of ongoing research in developing a content-based image retrieval system for biomedical images that supports text and image based queries. Also it uses the extracted image features to detect the pathology in the vertebrae that have been found to be repetitively and consistently detectable. Future work in this area focuses on automated detection of disc space narrowing,subluxation and spondylolisthesis. Additionally, these classifiers need to be included in the working system to enable intelligent retrieval of biomedical information from the NHANES data set.

REFERENCES

[1] S. Antani, R. Kasturi, and R. Jain, "A survey on the use of pattern recognition methods for abstraction, indexing and retrieval of images and video," *Pattern Recognition*, vol. 35, no. 4, pp. 945–965, 2002.

[2] S. Antani, L. R. Long, and G. R. Thoma, "A biomedical information system for combined content-based retrieval of spine x-ray images and associated text information," in *To appear in Proceedings of the Indian Conference on Computer Vision, Graphics, and Image Processing*, 2002.

[3] L. R. Long and G. R. Thoma, "Image query and indexing for digital x-rays," in *Proceedings of IS&T/SPIE Conference on Storage and Retrieval for Image and Video Databases VII, Vol. SPIE 3656*, San Jose, CA, January 1999, pp. 12–21.

[4] L. R. Hedlund and J. C. Gallagher, "Vertebral morphometry in diagnosis of spinal fractures," *Journal of Bone Mineral Research*, vol. 5, pp. 59–67, 1988.

[5] R. Eastell, S. L. Cedel, H. W. Wahner, B. L. Riggs, and L. J. Melton, "Classification of vertebral fractures," *Journal of Bone Mineral Research*, vol. 6, pp. 207–215, 1991.

[6] R. Smith-Bindman, S. R. Cummings, P. Steiger, and H. K. Genant, "A comparison of morphometric definitions of vertebral fracture," *Journal of Bone Mineral Research*, vol. 6, pp. 25–34, 1991.

[7] P. D. Ross, J. W. Davis, R. S. Epstein, and R. D. Wasnich, "Ability of vertebral dimensions from a single radiograph to identify fractures," *Calcif Tissue Int*, vol. 51, pp. 95–99, 1992.

[8] S. Ott, R. Kilocyne, and C. H. Chesnut III, "Ability of four different techniques of measuring bone mass to diagnose vertebral fractures in postmenopausal women," *Journal of Bone Mineral Research*, vol. 2, pp. 201–210, 1991.

[9] T. J. A. and D. Resnick, "The aging spine: radiographic-pathologic correlatio," in *Vertebral Fracture in Osteoporisis*, H. K. Genant, M. Jergas, and C. van Juijk, Eds. San Francisco: Osteoporosis Research Group, University of California at San Francisco, 1995, ch. 4.

[10] R. J. Stanley and L. R. Long, "A radius of curvature-based approach to cervical spine vertebra image analysis," in 38th *Annual Rocky Mountain Bioengineering Symposium*, vol. 37, 2001, pp. 385–390.

[11] M. Kass, A. Witkin, and D. Terzopoulos, "Snakes: Active contour models," *International Journal of Computer Vision*, vol. 1, no. 4, pp. 321–331, 1988.

[12] T. F. Cootes and C. J. Taylor, "Statistical models of appearence for computer vision," University of Machester, Wolfson Image Analysis Unit, Imaging Science and Biomedical Engineering, University of Manchester, Manchester, M12 9PT, U.K., Tech. Rep., February 2001.

[13] L. R. Long and G. R. Thoma, "Landmarking and feature localization in spine x-rays," *Journal of Electronic Imaging*, vol. 10, no. 4, pp. 939–956, 2001.

[14] N. Otsu, "A threshold selection method from gray-level histograms," *IEEE Transactions on Systems, Man, and Cybernetics*, vol. 9, no. 1, pp. 62–66, 1979.

[15] R. Gonzalez and R. Woods, *Digital Image Processing*, 2nd ed. Prentice Hall, 2002.